Integrated Ionic Flow Device and Heat Sink as a Fan Sink Alternative

Michael S June, James Kribs and Kevin M. Lyons

Department of Engineering & Technology,
Western Carolina University
Cullowhee, NC 28723
Phone: (1) 828-227-2564
Email: msjune@email.wcu.edu

Abstract - The norm for component cooling in the server industry today is passive heat sinks utilizing system level airflow. While the larger fans supplying the air flow can be made very efficient, they typically consume large amounts of power. Ionic air moving devices are under investigation in many industries, including the computer industry, as a low power alternative. Ionic devices are not capable of the same high-velocity airflows as axial fans and blowers, but have the advantage of being made part of the heat sink, providing sufficient localized flow. A small axial fan supplying local air flow to a heat sink was compared to an ionic device incorporated into the heat sink to compare power consumed, while cooling a simulated component to a reasonable temperature. It was shown that the ionic device provided the same cooling for an input of 0.17 W compared to the fan at 0.40W. Local cooling represents a paradigm shift from system level cooling, but these data show that in this new paradigm, the ionic devices can provide cooling at lower power input than conventional axial fans.

I. INTRODUCTION

Passive cooling of heated electronic devices is currently the norm in server and mainframe-type computers. The heat sinks take advantage of system-level air flow provided by larger fans at the inlet and/or outlet side of the system enclosure. While these fans can be made very efficient (35 – 40% static efficiency) they consume much more power than smaller, less-efficient fans often seen on fan sinks. It is difficult to compare the efficiency of a large fan providing system level flow to a smaller fan providing localized flow since the system level fan would likely be cooling more than one component, but given the inherent flow length losses between the larger fans and the heated components, it is easy to imagine scenarios which these losses would dominate the overall efficiency, rendering the system as a whole less efficient that a system cooled with active-, and therefore locally-cooled, fan sinks.

Ion driven air moving devices are under investigation in many industries including the computer industry. Their lack of moving parts and nearly silent operation offer an attractive alternative to the turbulent and noisy flow from conventional rotary AMDs. Comparing static efficiency, as well as airflow and back pressure, between the ionic devices and rotary devices shows significant disadvantages to the ionic devices. They provide less airflow, and much less pressure at lower efficiency. One key difference

between the devices is that the ionic device can be incorporated directly into the heat sink, thus rendering the efficiency comparison invalid. What matters is how much power can be cooled for a given energy input to the air moving device. The current study compares a small fan sink to the same heat sink with an integrated ionic device.

An ionic air moving device is characterized by the breakdown of air into ions in the presence of a high electric potential and an electrode with a high curvature. The ions then flow across the potential gradient. Momentum transfer between the ions and the air molecules result in airflow. Investigations of ion-driven gas flows are ongoing in such fields as electronics cooling [1], combustion in microgravity [2, 3] where the flame is the ion source, extinguishant dispersion [4], control of soot in flames and filtration [5]. The common structure across these applications is a thin cathode, such as a small diameter wire or a needle, and a larger anode. The anode can be a flat plate, which is typically paired with the wire type cathode (Figure 1), or a ring anode paired with a needle cathode (Figure 2). In the current study the anode, sometimes referred to as the collector, was a heat sink.
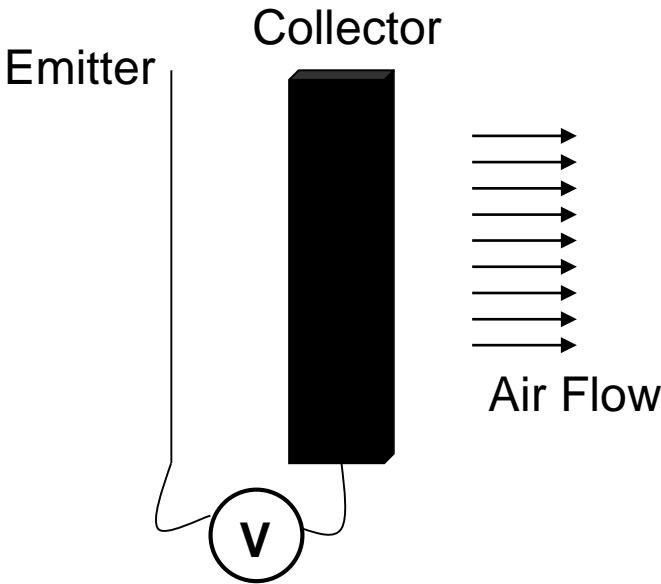

Figure 1. Schematic of an ionic air moving device consisting of a wire electrode and a plate electrode.
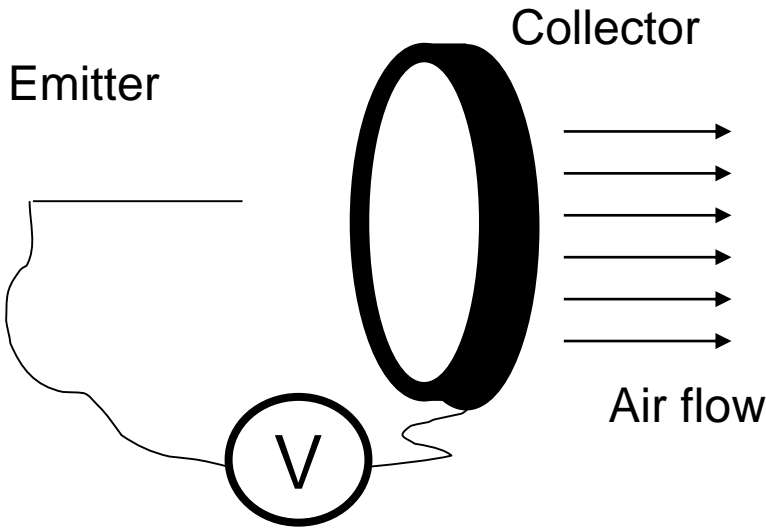
Figure 2. Schematic of an ionic air moving device consisting of a pin or needle electrode and a ring electrode.

These flows have been documented since before 1709 as mentioned in a review paper by Robinson [6], but the first well documented work was considered to be by Chattock [7] in 1899. Weinberg, and Dunn-Rankin [2, 3, 4, 8, 10] have previously demonstrated improvements in flow rate, back pressure, and optimizations in geometry over earlier work, and have done much to demonstrate the viability of this technology. The physics behind these flows has been well studied and characterized. A thorough treatment is given in [3, 9, 10, 16, 17].

Ionic flows are often characterized by which electrode is positive and which is negative. If the source electrode is positive, it is characterized as a positive ionic flow, and conversely if it is negative, the flow is a negative ionic flow. Chen and Davidson found that negative ionic flows have higher velocities than positive ionic flows [11]. This result was also reported by Moreau et al [12], and Tsubone et al [13]. Komeili et al [14] compare the flow profiles of positive and negative ionic flows, as well as concluding that negative ionic flows had higher flow than positive ionic flows.

Many researchers have looked at providing, localized enhancement of flows using ionic devices. Yue et al. [18] reported using ion driven devices to enhance the air flow on to a specific electronic device, rather than to cool with a system level airflow in the conventional sense. The current literature [1, 8, 9] suggests that ionic air moving devices are not capable of generating large system level airflows, however there has been some success reported cooling a laptop computer [19], which typically employs local cooling with rotary devices.

Efficiency is discussed in several papers [8, 12, 15, 16, 17], however few attempts have been made to compare conventional fan sinks to heat sink integrated ionic devices.

II. PROCEDURE

A small aluminum extruded profile heat sink was placed on a circular cartridge heater, and placed in a flow bench. The overall dimensions of the heat sink were 31 mm length x 31 mm wide x 28 mm tall with a base thickness of 2 mm (26 mm tall fins). There were 12 fins, each 0.9 mm thick with 2mm spacing. There was a 4 mm space between the center two fins. Air flow to the heat sink was provided by either a 25 mm axial fan, or by integrating an ionic airflow device. The ionic device consisted of 5 common 3 mm sewing needles as shown in Figure 3.
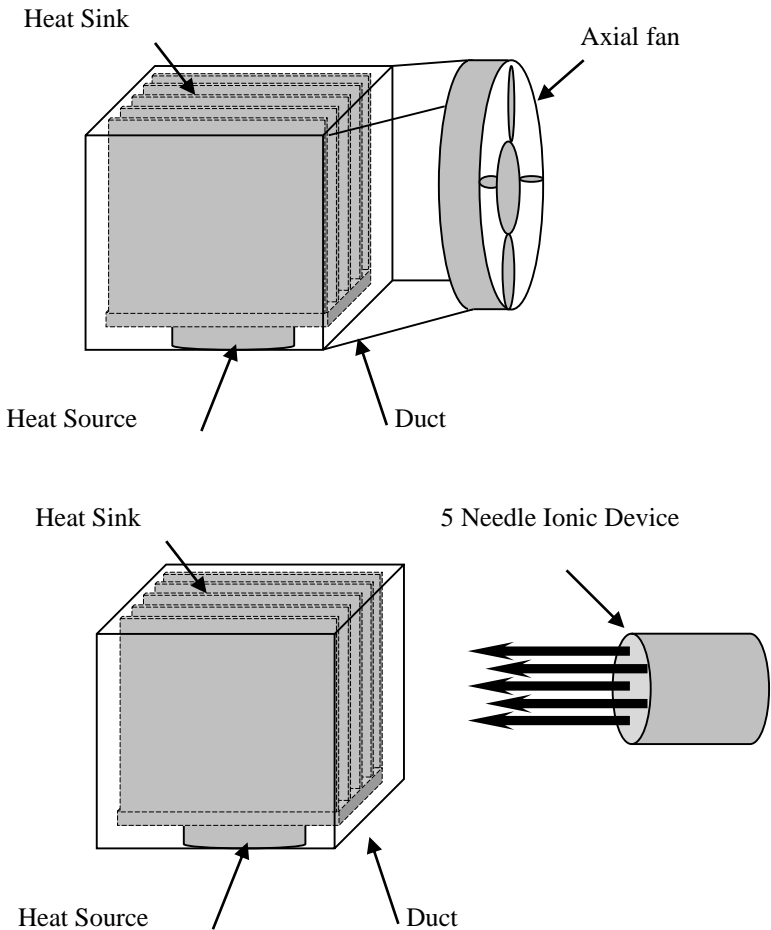

Figure 3. Sketch of the heat sink ducted to the axial fan, and the heat sink as part of a 5 needle ionic air moving device.

A 20kV Acopian DC power supply was used to supply a potential between the needle and the heat sink for the ionic device. For negative ionic flow, negative potential was applied to the needles, and the aluminum heat sink was grounded. For positive ionic flow, the negative potential was applied to the heat sink, and the needles were grounded.

Air flow was measured using a flow bench consisting of an air flow source and a chamber. Air flow through the chamber was balanced with air flow from the ionic air moving device by closing a valve between the air flow source and the chamber. When static pressure in the chamber was zero, the air flow into the chamber from the ionic device was the same as the air flow out of the chamber from the air flow source. Static pressure was measured with a Setra 339-1 digital manometer. Volumetric air flow was measured with a Miriam 50MW20-1F linear flow element and a Datametrics 1018 differential manometer.

At each point, voltage and current to the ionic air moving device were measured. These data were used to generate the P-Q curves used to determine static efficiency. Voltage to the ionic device was measured using a Hewlett Packard HP3468A DMM attached to the voltage sense terminals of the Acopian power supply. Current was measured also using a Hewlett Packard HP3468A DMM attached to the current sense terminals on the Acopian power supply. The offset for voltage readings was 1 V indicated for 10,000 V output. For the current measurement, 1 V indicated 1 mA output.

Since efficiency is a function of distance between the emitter and the collector, this distance was varied from 11 mm to 35 mm and static efficiency was determined at seven increments to determine the optimal distance.

Heat was applied to the heat sink using a 19 mm diameter circular heater with thermal grease between the heater and the heat sink. The heat sink base temperature was measured with a thermocouple when evaluating the fan.

The fan was fully ducted to the heat sink when placed on the flow bench. The fan was powered up along with the heater, and the temperature of the heat sink base in the middle of the heater was measured with the thermocouple. The airflow through the heat sink was measured using the flow bench, and the power used by the fan was noted. The fan was then removed, and the 5 needle ionic device was assembled, and powered to the same airflow as the fan. Power used by the ionic airflow device was measured by noting the voltage and current drawn by the device.

III. RESULTS

With the axial fan at full speed, fully ducted to the heat sink, the thermal resistance from the base to the air was 1.9 C/W. This was achieved with the fan consuming 0.4W of electrical power. The airflow through the heat sink was 462 cm^3/s (0.98 SCFM). The heater supplied 17W of power.

Figure 4 shows the static efficiency of the ionic device using the heat sink as the collector, for various needle to heat sink distances. Based on these data, the needles were placed 21 mm in front of the heat sink for both the positive and negative ionic device.

The 5 needle positive ionic device consumed only 0.19 W at 462 cm^3/s through the heat sink. Subsequently the device was reconfigured as a negative ionic device and was tested at 462 cm^3/s, consuming 0.17W as shown in Table 1.
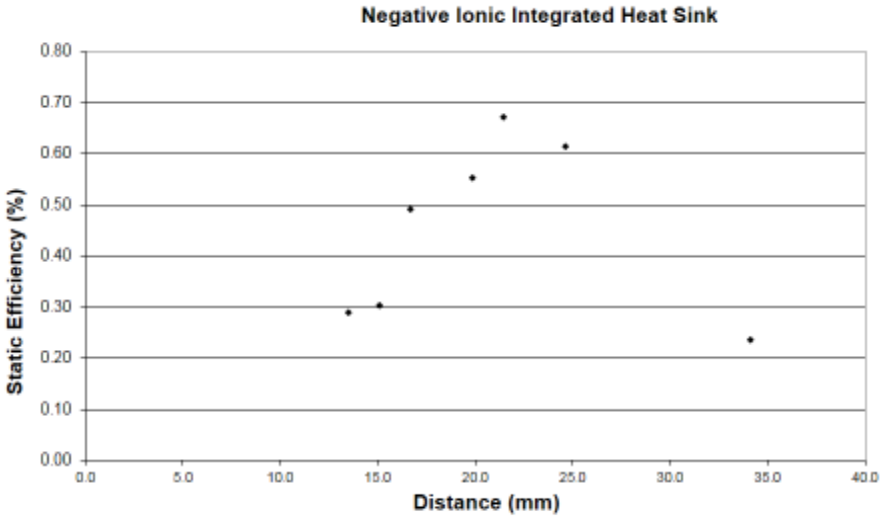
Negative Ionic Integrated Heat Sink

Figure 4. Static efficiency as a function of distance between the needle and the heat sink. Static efficiency peaks at a distance of 21 mm between the needles and the heat sink.

Table 1. Comparison of power consumed by each air moving device at 462 cm^3/s air flow.

Device	Airflow	Power
	(cm^3/s)	(W)
25 mm Axial Fan/ Heat Sink	462	0.40
Positive Ionic Device/ Heat Sink	462	0.19
Negative Ionic Device/ Heat Sink	462	0.17

IV. DISCUSSION

The ionic devices both consumed less power than the fan when cooling a simulated low power electronic component at 17W heat output. In computer systems, devices of concern in this power range generally have to be kept below 85C at the silicon level. The temperature at the heat sink base is typically 70C when the silicon is at 85C, assuming typical thermal resistances from the silicon to the point of measurement on the heat sink base. Heat sink base temperature was measured only for the axial fan cooled heat sink due to difficulties with thermocouple measurement and ionic devices. The negative ionic device induces enough voltage in the thermocouple wire to cause significant inaccuracy. Since the needles were grounded on the positive ionic device, the thermocouple would have been at the same high potential as the heat sink, rendering it unreadable in that case as well. For these reasons, airflow was held constant between the three cases, and the assumption was made that the heat sink base temperature would be the same given the same airflow, ambient conditions, and heater power. The uncertainty of the power measurements was less than 0.2%. The instrumentation used was calibrated within the previous 6 months to NIST traceable standards. Because the airflow measurement was for reference, and was held constant it was deemed acceptable to use uncalibrated instrumentation.

V. CONCLUSIONS

The results of this study show the ionic air moving device used less power than a comparable axial fan to cool a low power electronic component.

1) At 462 cm^3/s (0.98 SCFM), the negative ionic AMD required 0.17W while the axial fan required 0.40W
2) The negative ionic device consumed slightly less power than the negative device (0.17 W vs. 0.19 W) at equivalent airflow, but both consumed less than half the power as the fan.
3) The stated flow conditions and heat sink were sufficient to cool at 17W component to a reasonable temperature of 70C at an ambient condition of 35C and 3000ft altitude. This is a typical upper bound for computer equipment.

REFERENCES

[1]   D. Go, S. V. Garimella, T. S. Fisher, and R. K. Mongia, Ionic Winds for Locally Enhanced Cooling, J. Appl. Phys. 102 (2007) 053302

[2]   F. Weinberg, F. Carleton, D. Dunn-Rankin, Electric Field-Controlled Mesoscale Burners, Combust. Flame 152 (2008) 186

[3]   B.A. Strayer, J.D. Posner, D. Dunn-Rankin, F.J. Weinberg, Simulating Microgravity in Small Diffusion Flames by Using Electric Fields to Counterbalance Natural Convection, Proc. R. Soc. London Ser. A 458 (2002) 1151

[4]   F.J. Weinberg, F.B. Carleton, D. Dunn-Rankin, Development of Electrically Charged Extinguishant Dispersions for use in Microgravity, Combustion Science and Technology, 175 12 (2003) 2161

[5]   S.C. Saxena, R.F. Henry, W.F. Podolski, Technology Status of Particulate Removal From High-Temperature High-Pressure Combustion Gases, Aerosol Sci. Technol., 1 2 (1982) 235

[6]   M. Robinson, Movement of Air in the Electric Wind of the Corona Discharge. Trans. Am. Inst. Elec. Eng. 80 (1961) 143

[7]   A. P. Chattock, On the Velocity and Mass of Ions in the Electric Wind in Air. Philos. Mag. S 548 294 (1899) 401

[8]   M. Rickard, D. Dunn-Rankin, F. Weinberg, F. Carleton, Maximizing ion-driven gas flows, J. Electrostat. 64 (2006) 368

[9]   L. Zhao, K. Adamiak, EHD Flow in Air Produced by Electric Corona Discharge in Pin-Plate Configuration, J. Electrostat. 63 (3-4) (2005) 337

[10] D. Dunn-Rankin, F.J. Weinberg, Using Large Electric Fields to Control Transport in Microgravity, Proceedings of the Interdisciplinary Transport Phenomena in Microgravity and Space Sciences Conference IV, Tomar, Portugal, August 7-12, 2005

[11] J. Chen, J.H. Davidson, Model of the Negative DC Corona Plasma: Comparison to the Positive DC Corona Plasma, Plasma Chem. Plasma Process. 23 (2003) 83

[12] Eric Moreau, Gerard Touchard, Enhancing the Mechanical Efficiency of Electric Wind in Corona Discharges, J Electrostat. 66 (2008) 39

[13] H. Tsubone, J. Ueno, B. Komeili, S. Minami, G.D. Harvel, K. Urashima, C.Y. Ching, J.S. Chang, Flow Characteristics of DC Wire-Non-Parallel Plate Electrohydrodynamic Gas Pumps, J Electrostat. 66 (2008) 115

[14] B. Komeili, J.S. Chang, G. Harvel, Polarity Effect and Flow Characteristics of Wire-Rod Type Electrohydrodynamic Gas Pump, 2006 Annual Report on Electrical Insulation and Dialectric Phenomena, (2006) 182

[15] C. Kim, D. Park, K.C. Noh, J. Hwang, Velocity and Energy Conversion Efficiency Characteristics of Ionic Wind Generator in a Multistage Configuration, Journal of Electrostatics 68 (2010) 36

[16] H. Bondar, F. Bastien, Effect of Neutral Fluid Velocity on Direct Conversion from Electrical to Fluid Kinetic Energy in an Electro Fluid Dynamics (EFD) Device, J. Phys. D. Appl. Phys., 19 (1986) 1657

[17] M. Goldman, A. Goldman, R.S. Sigmond, The Corona Discharge, Its Properties and Specific Uses, Pure Appl. Chem., 57 (1985) 1353

[18] Y. Yue, J. Hou, Z. Ai, L. Yang, Q. Zhang, Experimental studies of the enhanced heat transfer from a heating vertical flat plate by ionic wind, Plasma Science and Technology, Vol. 8, No.6, (2006) 697